
Is A Picture Worth A Thousand Words? Delving Into Spatial Reasoning for Vision Language Models

Jiayu Wang¹ Yifei Ming¹ Zhenmei Shi¹ Vibhav Vineet² Xin Wang² Neel Joshi²
¹University of Wisconsin–Madison ²Microsoft Research
{jwang2782, ming5, zshi89}@wisc.edu, {vivineet, wanxin, neel}@microsoft.com

Abstract

Large language models (LLMs) and vision-language models (VLMs) have demonstrated remarkable performance across a wide range of tasks and domains. Despite this promise, spatial understanding and reasoning—a fundamental component of human cognition—remains under-explored. We develop novel benchmarks that cover diverse aspects of spatial reasoning such as relationship understanding, navigation, and counting. We conduct a comprehensive evaluation of competitive language and vision-language models. Our findings reveal several counter-intuitive insights that have been overlooked in the literature: (1) Spatial reasoning poses significant challenges where competitive models can fall behind random guessing; (2) Despite additional visual input, VLMs often under-perform compared to their LLM counterparts; (3) When both textual and visual information is available, multi-modal language models become less reliant on visual information if sufficient textual clues are provided. Additionally, we demonstrate that leveraging redundancy between vision and text can significantly enhance model performance. We hope our study will inform the development of multimodal models to improve spatial intelligence and further close the gap with human intelligence.

1 Introduction

The recent breakthroughs in foundation models have had a transformative effect on research and industry, and we have seen these models rapidly integrated into products and new businesses that are shaping people’s lives for the better. This sea change was initially driven by large language models (LLMs), which have shown at times near unbelievable, human-level performance across a wide range of tasks. Over the past year, many of these models have been extended to handle images in addition to text, leading to a significant increase in vision-language models (VLMs), especially multimodal large language models (MLLMs), which demonstrate groundbreaking performance in image-related tasks as in the text domain.

However, the reality is not quite as rosy as advertised. While these models have been instrumental in advancing the state-of-the-art in complex reasoning tasks such as common sense reasoning, mathematical problem solving, and scientific question answering [17, 28, 38, 66, 69], they have not been as effective for a number of problem domains. In particular, as we will show in this paper, they have limited performance on tasks that require detailed visual understanding and reasoning of images.

Visual understanding and reasoning—an intrinsic part of human perception and cognitive ability—has been largely under-explored when it comes to VLMs. In fact, it is often argued that the visual sense is the dominant sense in people, yet when it comes to current models, it seems quite secondary. Spatial reasoning, in particular, is fundamental to everyday human activities such as navigating environments, understanding maps, and manipulating objects. It encompasses skills that are crucial for both survival and higher-order cognition, including the ability to navigate through space, recognize patterns, and deduce relationships from spatial configurations.

In this paper, we develop three novel, visual-question answering (VQA) style benchmarks (Spatial-Map, Maze-Nav, and Spatial-Grid, details in Section 3.1) to explore the performance

of VLMs on diverse aspects of spatial reasoning, including relationship, navigation, position understanding, and object counting. Humans excel at such tasks, making them essential capabilities for intelligent systems to emulate for safe and effective deployment in the real world.

Our dataset, however, is constructed with a key twist – each problem in our benchmark has an image and a text representation that is sufficient for answering each spatial understanding question. We denote the use of these sources as VQA, which is the standard task of visual-question answering that consists of a vision-only input and a question, TQA, text-only input and a question, and VTQA, a combination of the previous with vision and text input.

We conduct a systematic and comprehensive evaluation on a wide range of open-source and proprietary LLMs and VLMs. We perform in-depth analysis and unveil several novel and surprising results that challenge the current understanding of how these models handle spatial information:

- **Spatial reasoning remains challenging:** VLMs frequently struggle with spatial reasoning tasks, with some competitive models performing worse than random guessing.
- **Visual vs. textual inputs:** Without detailed textual descriptions, multimodal models rarely surpass the performance of their LLM backbones when relying solely on visual inputs. This underscores the critical role of text in enhancing model performance on spatial reasoning.
- **Reduced reliance on visual information:** When both textual and visual inputs are provided, multimodal language models tend to rely less on the visual component if sufficient textual clues are available.
- **Textual performance of VLMs:** VLMs often outperform their LLM counterparts with text-only inputs, indicating that the language model backbones within VLMs benefit from multimodal training, despite a lack of similar benefits from the visual components.

We surmise that the limitations in spatial understanding of VLMs arise from the overly simplistic treatment of images in the current VLM architectures and training pipelines. We believe that the contributions in this paper will drive changes in how these models are constructed so that they can unlock greater spatial reasoning capabilities, bridging the gap to human-like intelligence.

2 Related Work

Large language models. The generative large language models (LLMs) have been successful in recent years, which are based on the transformer architecture introduced by [61]. These LLMs, such as BERT [14], OPT [70], PaLM [12], Gemma [56], Mistral [25], GPT-3 [10], GPT-4 [2], Claude3 [5], Grok-1 [63], Llama [58], Llama2 [59], Llama3 [3] and so on, have profoundly changed the world due to their emergent ability, e.g., in-context learning [43, 45, 53], compositional ability [16, 19, 64] and adaptation ability [51, 52, 65]. LLMs have been involved in human activities, such as finance [31], bio-informatics [57], law [54], education [27], coding [23], and even creative writing [2] such as top AI conference reviews [33].

Large vision-language models and multi-modality. The success of LLMs has propelled the adoption of the transformer architecture within the computer vision community, such as ViT [15], Beit [9], CLIP [48], MAE [20], Swin [39, 40] and DiT [47]. Building on the capabilities of powerful LLMs, multi-modal language models (MLLMs) such as Flamingo [4], LLaMA-Adapter [18, 68], LLaVA [34, 36], stable-diffusion [49], BLIP [29, 30], MiniGPT-4 [71], Qwen [7, 8], Gemini [55], MM1 [42] have significantly expanded the scope of tasks that can be addressed. These models adeptly handle inputs from diverse modalities and have demonstrated remarkable performance on a wide range of tasks such as mathematical reasoning [41], visual question answering [6, 37], image-text retrieval [67], and visual reasoning [26].

Spatial understanding and reasoning. Spatial reasoning entails comprehending and manipulating spatial relationships, a task significantly more challenging than visual grounding [1, 26, 46]. Although progress in natural language processing, evaluations, and benchmarks on LLMs such as GPT-4 [2] and Claude3 [5] have predominantly focused on textual or relational reasoning. This focus often overlooks the intricate nature of spatial reasoning tasks. Notably, recent studies [17, 28, 38, 44, 50, 66, 69] have conducted thorough evaluations across a diverse range of tasks. Yet, they demonstrate a scant exploration of spatial reasoning capabilities, highlighting a gap in assessing this complex cognitive skill in current benchmarks. In particular, Zhang *et al.* [69] suggest that MLLMs primarily leverage

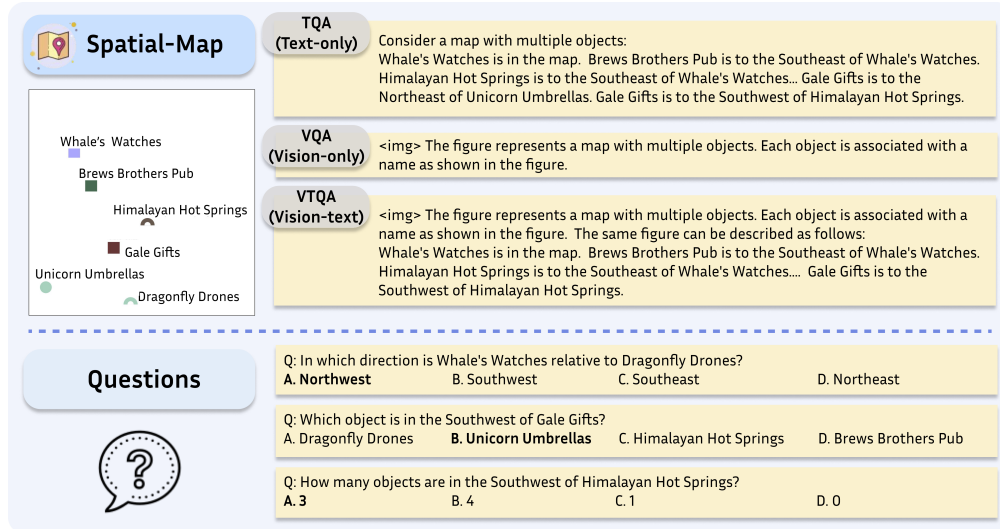


Figure 1: Illustration of the Spatial-Map task, which simulates a map with multiple locations. To investigate the impact of modality, we consider three input formats: Text-only, Vision-only, and Vision-text. We evaluate language models (w. Text-only input) and multimodal language models (w. Vision-only and Vision-text inputs) on the same set of questions.

textual cues rather than visual diagrams to solve math problems while focusing only on math problems. Yamada *et al.* [66] design simple navigation tasks and finds LLMs appear to capture certain aspects of spatial structure implicitly, but room for improvement remains, while our benchmarks are more complicated than their navigation tasks based on simple geometry maps. Fu *et al.* [17] propose a benchmark on science and games with limited exploration related to spatial reasoning, while we are dedicated diverse spatial reasoning tasks with in-depth analysis.

3 Dataset and Task Construction

3.1 Dataset Setup

To evaluate the spatial reasoning abilities of LLMs and VLMs, we construct three diverse tasks including spatial relationships, navigation, position understanding, and counting. To systematically study the impact of modality, we design three types of input prompts for each task: (1) Text-only: the input is purely textual and contains all necessary information for a person to answer the questions. (2) Vision-only: the input consists solely of an image, which provides sufficient details for a person to easily answer, a format also referred to as Visual Question Answering (VQA) in the literature. (3) Vision-text: the input includes both an image and its textual representation with detailed descriptions, rendering the information in both modalities redundant. We evaluate language models using Text-only inputs and multimodal language models using Text-only, Vision-only, and Vision-text inputs on the same set of questions. We opt for synthetic data in this work. Synthetic data offers several compelling advantages: (1) Avoidance of data leakage—since large language models are pre-trained on web-scale data, it is crucial to ensure that the test data have not been seen during training; (2) configurability—being fully configurable allows for controlled experiments and can be extended to additional tasks; (3) scalability—it is easy to scale the number of test samples, which enhances the statistical significance of our results.

Spatial-Map. Understanding the spatial relationships among objects on a map is a fundamental aspect of human cognitive abilities. To simulate this environment, we create a map-like dataset termed Spatial-Map with K objects, where K is configurable. Each object is associated with a unique location name, such as Unicorn Umbrellas and Gale Gifts. To study the impact of modality, the textual representation of each input consists of pairwise relations such as Brews Brothers Pub is to the Southeast of Whale's Watches. An example with $K = 6$ is shown in Figure 1, with Text-only, Vision-only, and Vision-text inputs. These questions include asking about the spatial relationships between two locations and the number of objects that meet specific spatial criteria.

Maze-Nav

TQA (Text-only)
 Here is a Maze represented in ASCII code (LHS) where the symbols have the following meanings: # represents walls that are impassable barriers. " " (space) represents the navigable path within the maze, ... A right turn is defined as a change in movement direction that is 90 degrees clockwise relative to the previous direction. A left turn is defined as a change in movement direction that is 90 degrees anticlockwise relative to the previous direction.

```
#####
#SXXX#
#XXXX#
#XXXX#
#EXXX#
#####
```

VQA (Vision-only)
 The figure represents a Maze, where the colored blocks have the following meanings: Black blocks represent walls that are impassable barriers. White blocks represent navigable paths within the maze, but not necessarily the correct path to the exit... A right turn is defined as a change in movement direction that is 90 degrees clockwise relative to the previous direction...

VTQA (Vision-text)
 The figure represents a Maze, where the colored blocks have the following meanings: Black blocks represent walls that are impassable barriers...The same Maze can be represented in ASCII code(LHS)... A right turn is defined as a change in movement direction that is 90 degrees clockwise relative to the previous direction. A left turn is defined as a change in movement direction that is 90 degrees anticlockwise relative to the previous direction.

```
#####
#SXXX#
#XXXX#
#XXXX#
#EXXX#
#####
```

Questions

?

Q: How many right turns are there in the provided path from S to E?
 A. 4 **B. 3** C. 7 D. 2

Q: How many total turns are there in the provided path from S to E?
 A. 4 B. 1 C. 9 D. 5

Q: Is the exit directly below the starting point, with no horizontal displacement?
 A. Yes B. No

Figure 2: Illustration of the Maze-Nav task, which evaluates the model’s ability to navigate from the starting point (S) to the exit (E). We consider three input formats: Text-only, Vision-only, and Vision-text. We evaluate language models (w. Text-only input) and multimodal language models (w. Vision-only and Vision-text inputs) on the same set of questions.

Maze-Nav. Navigation through complex spaces is essential for intelligent systems. To evaluate such abilities, we have developed a maze-like dataset named Maze-Nav. Visually, each sample can be represented as colored blocks where different colors signify distinct elements: a green block marks the starting point (S), a red block indicates the exit (E), black blocks represent impassable walls, white blocks denote navigable paths, and blue blocks trace the path from S to E. The objective is to navigate from S to E following the blue path, with movement permitted in the four cardinal directions (up, down, left, right). Alternatively, each input can be depicted in textual format using ASCII code. An example is illustrated in Figure 2, featuring Text-only, Vision-only, and Vision-text inputs. We construct this task based on an open-sourced library [24]. The questions asked include counting the number of turns from S to E and determining the spatial relationship between S and E. While such questions are easy for humans, we will show in Section 4 that they present significant challenges for modern multimodal language models.

Spatial-Grid. To investigate spatial understanding within structured environments, we introduce a grid-like dataset named Spatial-Grid, contrasting with the Spatial-Map where objects are positioned arbitrarily. Visually, each input consists of a grid of cells, each containing an image (*e.g.*, a rabbit). An example is illustrated in Figure 3. Alternatively, this grid can also be represented in a purely textual format; for instance, the first row might be described as: elephant | cat | giraffe | elephant | cat. The evaluations focus on tasks such as counting specific objects (*e.g.*, rabbits) and identifying the object located at a specific coordinate in the grid (*e.g.*, first row, second column).

3.2 Models

We consider a wide range of competitive open-sourced language models with different scales, including Phi2-2.7B [32], the LLaMA family of models (LLaMA-2-7B, LLaMA-2-13B, and LLaMA-3-8B) [60], Mistral-7B [25], the Vicuna family (Vicuna-7B-1.5 and Vicuna-13B-1.5) [11], and Nous-Hermes-2-Yi-34B. For multimodal language models, we consider the Bunny family (Bunny-Phi-2-SigLIP, Bunny-Phi-1.5-SigLIP, Bunny-Phi-2-EVA, and Bunny-Phi-1.5-EVA) [21], CogVLM [62], CogAgent [22], InstructBLIP family (InstructBLIP-Vicuna-7B and InstructBLIP-Vicuna-13B) [13], and LLaVA family (LLaVA-1.6-Mistral-7B, LLaVA-1.6-Vicuna-7B, LLaVA-1.6-Vicuna-13B, and LLaVA-1.6-34B) [35]. We also evaluate the proprietary models: Open AI’s GPT-4V, GPT-4O, GPT-4, Google Gemini Pro 1.0 and Anthropic Claude 3 Opus.

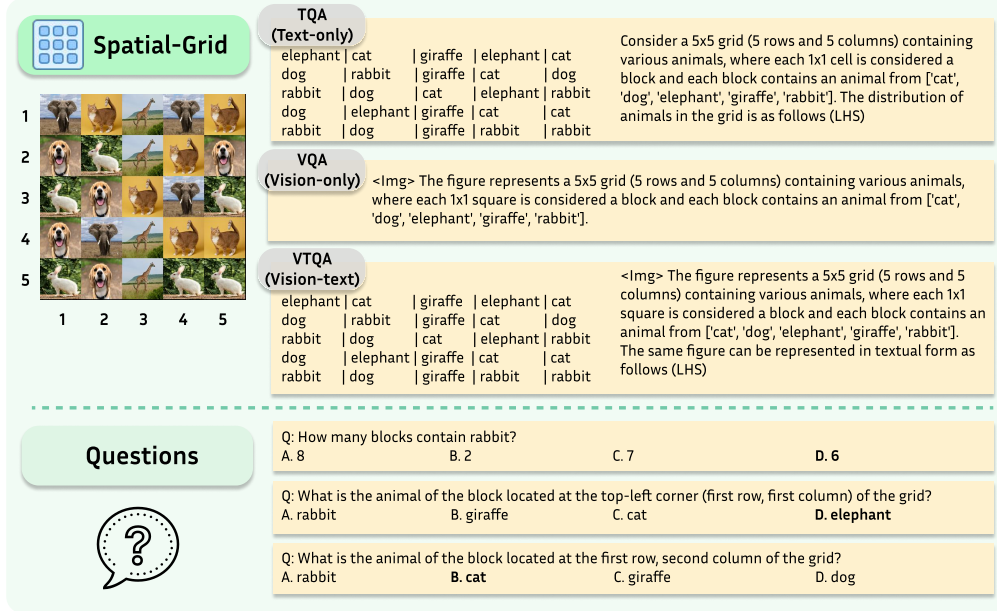


Figure 3: Illustration of the Spatial-Grid task, which evaluates the model’s spatial reasoning ability in a rigid grid structure. We consider three input formats: Text-only, Vision-only, and Vision-text. We evaluate language models (w. Text-only input) and multimodal language models (w. Vision-only and Vision-text inputs) on the same set of questions.

Evaluation. By default, 3 questions (termed Q1 to Q3) are associated with each sample in each task. As each question contains four options, we use accuracy as the main evaluation metric. The same user prompt is appended at the end of each question: *First, provide a concise answer in one sentence. Then, elaborate on the reasoning behind your answer in a detailed, step-by-step explanation.* For each model, we adopt the default configurations and decoding strategies, e.g., argmax for deterministic decoding and top- p for non-deterministic decoding. For non-deterministic decoding, the results are averaged over three independent runs for open-sourced models. For proprietary models, due to their limited availability and increased compute time and cost, we only used one run.

4 Main Results and Analysis

Spatial reasoning remains surprisingly challenging. The evaluation results on open-sourced models on Spatial-Map, Maze-Nav, and Spatial-Grid are shown in Figure 4. For each task, the reported accuracy is averaged over all questions. For vision-language models, we choose the Vision-only input format, commonly used in Visual Question Answering (VQA). We use a dashed red line in each figure to indicate the expected accuracy if answering by random guessing. Our findings reveal several notable insights: (1) Vision-only inputs: Despite the ease with which humans handle these tasks, most competitive multimodal language models perform at levels comparable to or barely above random guessing. (2) Text-only inputs: The textual representation includes essential spatial information. However, such input format generally does not enhance the spatial reasoning capabilities of competitive language models. An exception occurs in the Spatial-Grid task, where Llama-3 achieves an accuracy of 71.9%, followed by Mistral-7B-Instruct at 62.1%, both notably surpassing random guessing. Despite these successes, the performance of these models still lags significantly behind human levels. These results underscore the need for further development of techniques tailored to spatial understanding and reasoning.

The impact of input modality. To investigate the impact of modality, we compare the performance of a large language model (LLM) and a vision-language model (VLM) with the same language backbone. We consider the VQA (Vision-only) format for vision-language models. The results are shown in Figure 5. Each vertex on the spider plot represents the average accuracy of a (VLM, LLM) pair. We observe that on Spatial-Map and Spatial-Grid, the majority of VLMs yield worse performance compared to their LLM counterpart, despite having an additional visual encoder. For example, on

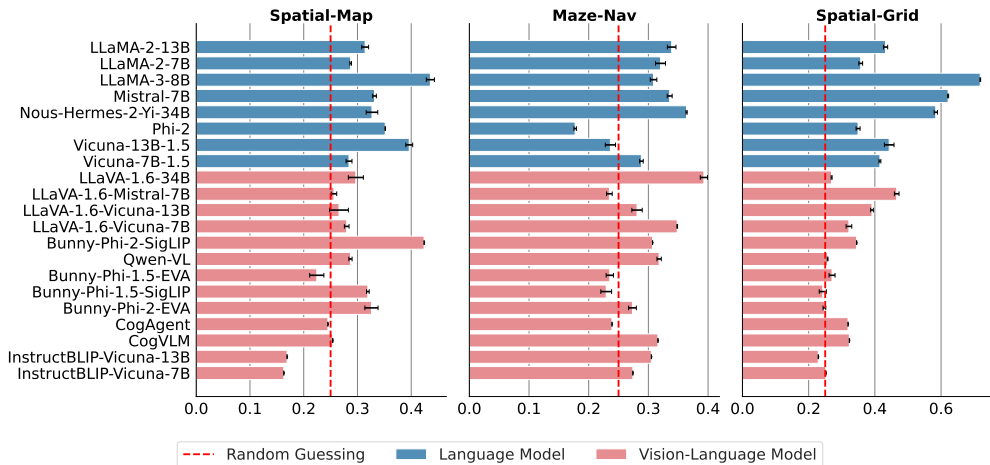


Figure 4: Performance overview on spatial reasoning tasks. We report the accuracy averaged over all questions. We consider the VQA (Vision-only) format for vision-language models. The dashed red line denotes the expected accuracy of random guessing. For *Spatial-Map* and *Maze-Nav* tasks, only a few models outperform random guessing by a notable margin.

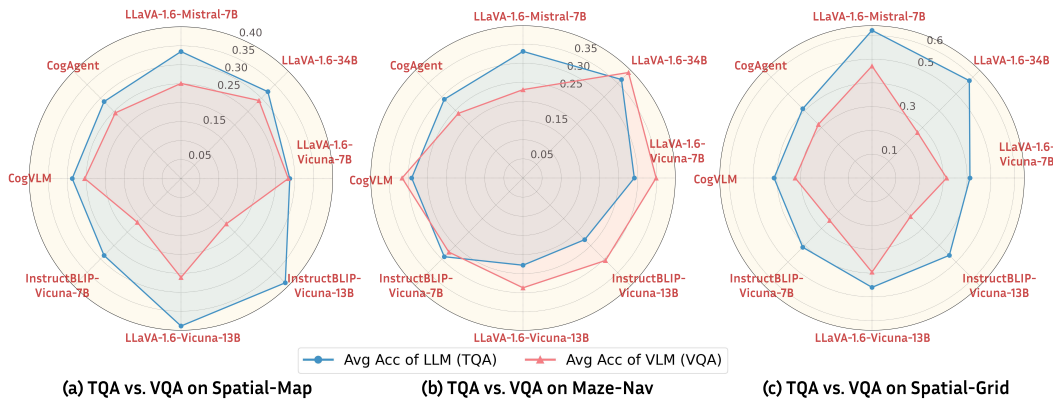


Figure 5: TQA vs. VQA on spatial reasoning tasks. Each vertex on the spider plot represents the Avg Acc of a (VLM, LLM) pair with the same language backbone, i.e., LLM v.s. VLM further finetuned on that. VLMs are depicted in red, and LLMs in blue. We can see that VLMs rarely enhance the performance compared to their LLM counterparts.

Spatial-Grid, *Mixtral-7B* achieves an average accuracy of 62.1%, while *LLaVA-v1.6-Mistral-7B* only yields an accuracy of 47.1% (15% ↓). Detailed results can be seen in Appendix D.

5 Delving Into Spatial Reasoning for Vision-Language Models

5.1 Seeing Without Understanding: The Blindness of Multimodal Language Models

To better understand how multimodal language models process visual information, we conduct a series of controlled experiments in the VTQA (Vision-text input) setting. For each sample, we replace the original image input (that matches the textual description) with either: (1) *No Image*: only keep the textual input without the image input, (2) *Noise Image*: a Gaussian noise image irrelevant to the task, and (3) *Random Image*: a random image from the dataset that does not match the textual description, as shown in Figure 6.

VLMs exhibit improved performance when visual input is absent. We conducted experiments by entirely removing the *Original Image* and relying solely on the textual description. The results are shown in Figure 7. For each task, we report the accuracy averaged across all questions. Remarkably,

the absence of visual input leads to better performance across a range of VLM architectures. For instance, the performance of LLaVA-1.6-34B on the `Spatial-Grid` task improved by 20.1% when no image was presented compared to scenarios with the original image. This observation underscores that when textual information alone can address the questions, additional visual inputs do not necessarily enhance, and may even hinder the performance, a sharp contrast to human capabilities where visual cues significantly aid in understanding. The removal of visual input forces the models to utilize the textual information to solve spatial reasoning tasks.

Noise image can improve the performance. We replace the *Original Image* with a *Noise Image* while retaining the original textual description. The results are shown in Figure 8. Consistent with the findings in *Original Image vs. No Image*, using a noise image also improves the performance across various VLM architectures. For example, the accuracy of LLaVA-1.6-Vicuna-13B increases by 6.5% on the `Maze-Nav` task when the noise image is used as opposed to the original image. In contrast to the ‘No Image’ setting, noise images provide limited visual cues. Nonetheless, the model tends to prioritize the textual information, especially when visual cues are not pertinent to the task.

Mismatched image-text does not necessarily hurt.

To build on previous findings, we further investigate the effects of replacing the *Original Image* with a *Random Image* (illustrated in Figure 6). Unlike a noise image, a random image is task-related but may provide conflicting information compared to the textual description. Intuitively, one might expect that such random images would degrade VLM performance due to contradictory cues. However, as demonstrated in Figure 9, this expectation does not always hold true. For instance, *Random Image* in the `Maze-Nav` task leads to improved performance across various VLM architectures. This outcome implies that VLMs are not heavily reliant on visual information, particularly when adequate textual clues are provided.



Figure 6: Illustration of *Random Image* and *Noise Image* for the example in Figure 2.

5.2 Leveraging Redundancy in Multimodal Inputs

Multimodal language models offer considerable versatility in handling multimodal inputs. While the visual input alone often provides sufficient details for humans to address spatial reasoning tasks with ease, we propose that VLMs significantly benefit from the inclusion of textual descriptions alongside visual data, even if this introduces substantial redundancy. We verify this hypothesis by comparing VQA (Vision-only input) and VTQA (Vision-text input) across diverse VLM architectures. The results are shown in Figure 10, where each vertex on the spider plot represents the average accuracy of a (*Vision-only*, *Vision-text*) pair based on the same VLM. For `Spatial-Map` and `Spatial-Grid`, we can clearly see that having the additional textual input (VTQA) enhances the performance compared to only using images (VQA) across different VLM architectures. This suggests that textual inputs improve the accuracy of spatial reasoning in VLMs. We further compare TQA and VTQA in Appendix C. Detailed results are included in Appendix D.

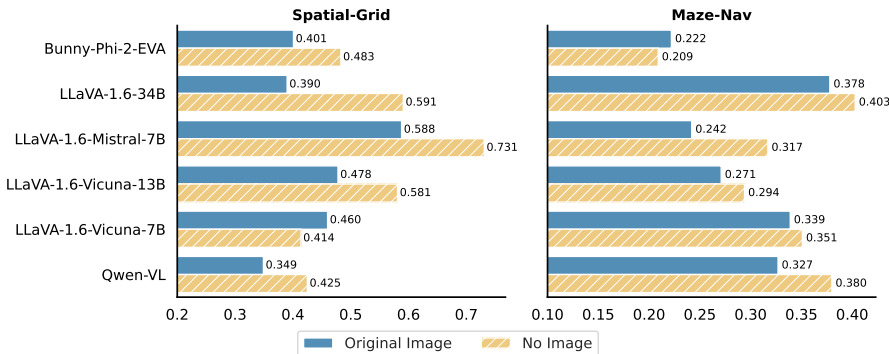


Figure 7: Original Image vs. No Image in VTQA. VLMs exhibit improved performance in spatial reasoning tasks when visual input is absent.

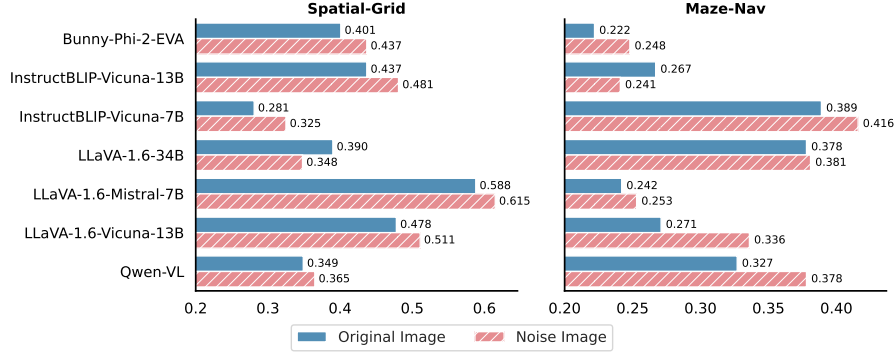


Figure 8: Original Image vs. Noise Image in VTQA. Replacing the original image with a Gaussian noise image improves the performance across diverse VLM architectures.

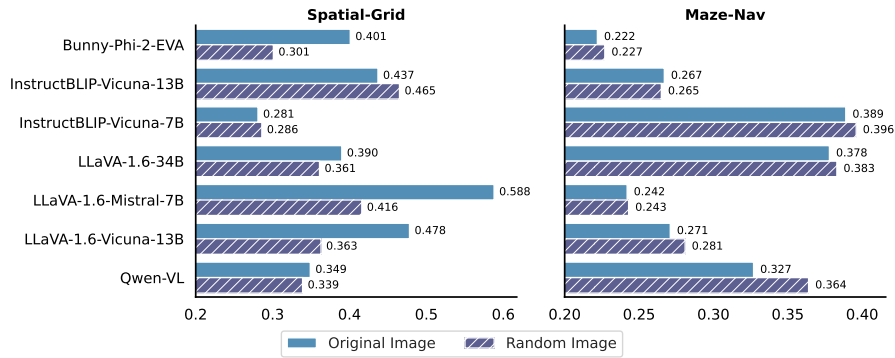


Figure 9: Original Image vs. Random Image in VTQA. On Maze-Nav, replacing the original image with a random image leads to performance improvement across diverse VLM architectures.

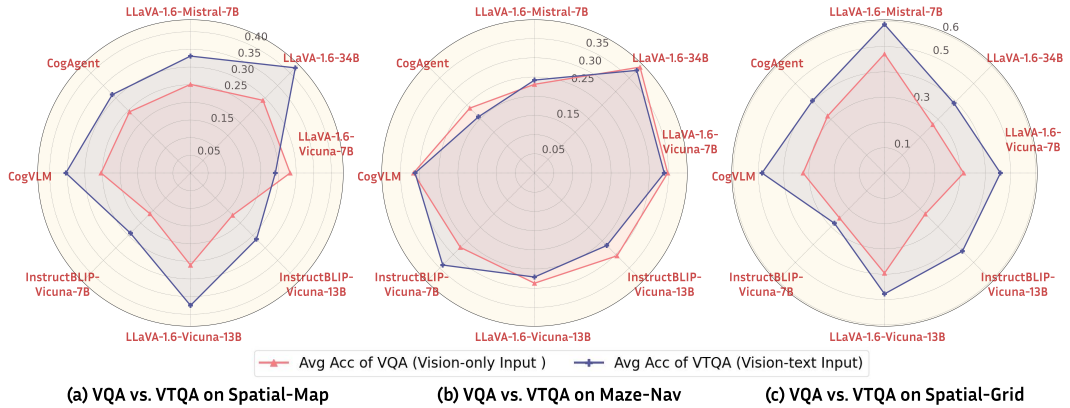


Figure 10: VQA vs. VTQA on spatial reasoning tasks. Each vertex on the spider plot represents the Avg Acc of a (Vision-only, Vision-text) pair with the same VLM model. We can see that having the additional textual input (VTQA) enhances the performance compared to only using images (VQA).

Text-only input with LLM vs. Text-only input with VLM. Given the demonstrated efficacy of text-only inputs, we conducted an ablation study to compare LLMs and VLMs using text-only inputs. We consider VLMs that are capable of processing text without accompanying visual data. The results are illustrated in Figure 11. Except for CogVLM, the majority of VLMs outperform their corresponding LLM backbones. This suggests that the language model backbones in VLMs demonstrate enhanced spatial reasoning abilities through multimodal learning. Conversely, the addition of visual information does not necessarily provide further benefits.

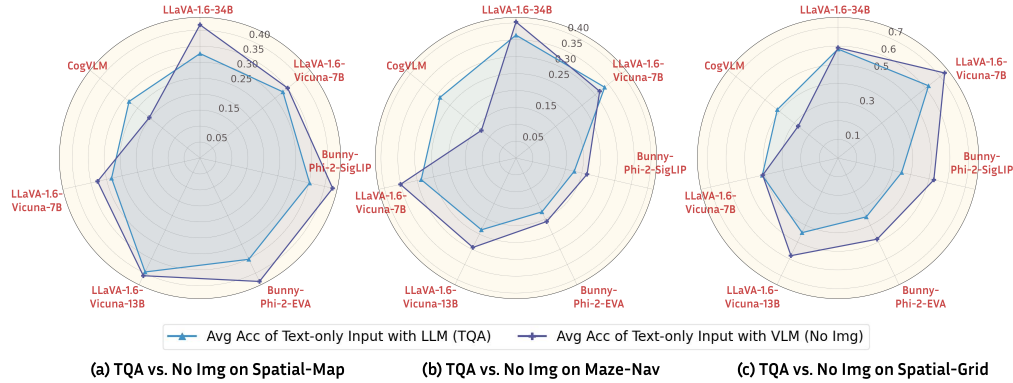


Figure 11: Comparison of Text-only input with LLM (TQA) vs. Text-only input with VLM (No Img). We consider VLMs that support text-only inputs. Each vertex on the spider plot represents the Avg Acc of a (LLM, VLM) pair with the same language model backbone.

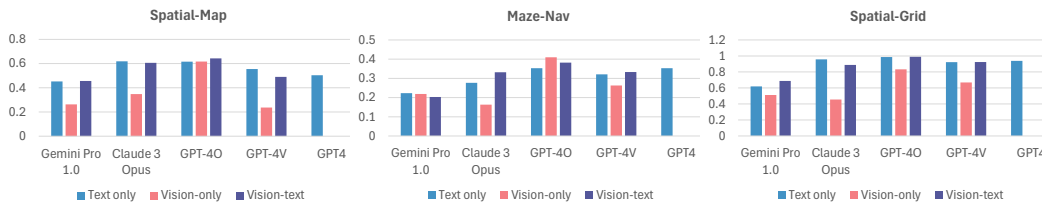


Figure 12: Results with proprietary models. Similar trends are observed as with open-source models.

5.3 Proprietary vs. Open-Source Models

As many recent benchmarks have shown that proprietary models generally outperform open-sourced models, it is important to understand if our observed trends hold with proprietary models. The performance of several top proprietary models (GPT-4, GPT-4V, GPT-4O, Gemini Pro 1.0, and Claude 3 Opus) are shown in Figure 12. We have the following salient observations: (1) A significant performance gap exists between SoTA open-sourced models and proprietary models, as expected. Furthermore, with both Text-only and Vision-text formats, GPT-4V and GPT-4O significantly outperform random guessing across all tasks. For instance, in the Vision-text format, GPT-4O achieves an accuracy of 0.989 on Spatial-Grid (Table 2). (2) Yet, the trends we observed with open source models hold, VQA consistently under-performs compared to TQA and VTQA, for example, GPT-4V’s performance improves by 25.6% on Spatial-Grid when switching from Vision-only to Vision-text input; and again no clear winner between TQA and VTQA (see Appendix C for further details), showing that proprietary models, even the new GPT-4O model, still do not appear to fully leverage visual inputs.

6 Discussion and Conclusions

We explored the spatial understanding capabilities of VLMs and LLMs. Our experiments resulted in several surprising conclusions across SoTA open-source and proprietary models. (1) VLMs struggle with spatial reasoning tasks (2) multimodal models rarely surpass LLMs when relying on visual inputs, (3) when both textual and visual inputs are provided, multimodal language models rely less on the visual inputs, and (4) VLMs often outperform their LLM counterparts with text-only inputs. This challenges the belief that current VLMs are highly performant at a wide range of vision-text tasks. However, with further thought, perhaps this is to be expected after all. The currently known architectures for VLMs attempt to “translate” the vision input into the language space and all reasoning is then performed in the language domain. It is logical that this automatic translation path is worse than a human provided translation to text, as in our text-only scenario. Thus our work shows the limits of the translation approach. Instead, to bridge the gap to human performance, future models require new architectures that treat vision input as a first-class source of information and reason in a joint vision-language space. It is our hope that our work informs development on this path.

References

- [1] Mostafa Abdou, Artur Kulmizev, Daniel Hershcovich, Stella Frank, Ellie Pavlick, and Anders Søgaard. Can language models encode perceptual structure without grounding? a case study in color. *arXiv preprint arXiv:2109.06129*, 2021.
- [2] Josh Achiam, Steven Adler, Sandhini Agarwal, Lama Ahmad, Ilge Akkaya, Florencia Leoni Aleman, Diogo Almeida, Janko Altenschmidt, Sam Altman, Shyamal Anadkat, et al. Gpt-4 technical report. *arXiv preprint arXiv:2303.08774*, 2023.
- [3] Meta AI. Introducing meta llama 3: The most capable openly available llm to date, 2024. <https://ai.meta.com/blog/meta-llama-3/>.
- [4] Jean-Baptiste Alayrac, Jeff Donahue, Pauline Luc, Antoine Miech, Iain Barr, Yana Hasson, Karel Lenc, Arthur Mensch, Katherine Millican, Malcolm Reynolds, et al. Flamingo: a visual language model for few-shot learning. *Advances in neural information processing systems*, 35:23716–23736, 2022.
- [5] Anthropic. The claude 3 model family: Opus, sonnet, haiku, 2024. https://www-cdn.anthropic.com/de8ba9b01c9ab7cbabf5c33b80b7bbc618857627/Model_Card_Claude_3.pdf.
- [6] Stanislaw Antol, Aishwarya Agrawal, Jiasen Lu, Margaret Mitchell, Dhruv Batra, C Lawrence Zitnick, and Devi Parikh. Vqa: Visual question answering. In *Proceedings of the IEEE international conference on computer vision*, pages 2425–2433, 2015.
- [7] Jinze Bai, Shuai Bai, Yunfei Chu, Zeyu Cui, Kai Dang, Xiaodong Deng, Yang Fan, Wenbin Ge, Yu Han, Fei Huang, et al. Qwen technical report. *arXiv preprint arXiv:2309.16609*, 2023.
- [8] Jinze Bai, Shuai Bai, Shusheng Yang, Shijie Wang, Sinan Tan, Peng Wang, Junyang Lin, Chang Zhou, and Jingren Zhou. Qwen-vl: A versatile vision-language model for understanding, localization, text reading, and beyond. *arXiv preprint arXiv:2308.12966*, 2023.
- [9] Hangbo Bao, Li Dong, Songhao Piao, and Furu Wei. Beit: Bert pre-training of image transformers. *arXiv preprint arXiv:2106.08254*, 2021.
- [10] Tom Brown, Benjamin Mann, Nick Ryder, Melanie Subbiah, Jared D Kaplan, Prafulla Dhariwal, Arvind Neelakantan, Pranav Shyam, Girish Sastry, Amanda Askell, et al. Language models are few-shot learners. *Advances in neural information processing systems*, 33:1877–1901, 2020.
- [11] Wei-Lin Chiang, Zhuohan Li, Zi Lin, Ying Sheng, Zhanghao Wu, Hao Zhang, Lianmin Zheng, Siyuan Zhuang, Yonghao Zhuang, Joseph E. Gonzalez, Ion Stoica, and Eric P. Xing. Vicuna: An open-source chatbot impressing gpt-4 with 90%* chatgpt quality, March 2023.
- [12] Aakanksha Chowdhery, Sharan Narang, Jacob Devlin, Maarten Bosma, Gaurav Mishra, Adam Roberts, Paul Barham, Hyung Won Chung, Charles Sutton, Sebastian Gehrmann, et al. Palm: Scaling language modeling with pathways. *Journal of Machine Learning Research*, 24(240):1–113, 2023.
- [13] Wenliang Dai, Junnan Li, Dongxu Li, Anthony Meng Huat Tiong, Junqi Zhao, Weisheng Wang, Boyang Li, Pascale N Fung, and Steven Hoi. Instructblip: Towards general-purpose vision-language models with instruction tuning. *Advances in Neural Information Processing Systems*, 36, 2024.
- [14] Jacob Devlin, Ming-Wei Chang, Kenton Lee, and Kristina Toutanova. Bert: Pre-training of deep bidirectional transformers for language understanding. *arXiv preprint arXiv:1810.04805*, 2018.
- [15] Alexey Dosovitskiy, Lucas Beyer, Alexander Kolesnikov, Dirk Weissenborn, Xiaohua Zhai, Thomas Unterthiner, Mostafa Dehghani, Matthias Minderer, Georg Heigold, Sylvain Gelly, et al. An image is worth 16x16 words: Transformers for image recognition at scale. *arXiv preprint arXiv:2010.11929*, 2020.

- [16] Nouha Dziri, Ximing Lu, Melanie Sclar, Xiang Lorraine Li, Liwei Jiang, Bill Yuchen Lin, Sean Welleck, Peter West, Chandra Bhagavatula, Ronan Le Bras, et al. Faith and fate: Limits of transformers on compositionality. *Advances in Neural Information Processing Systems*, 36, 2024.
- [17] Deqing Fu, Ghazal Khalighinejad, Ollie Liu, Bhuwan Dhingra, Dani Yogatama, Robin Jia, and Willie Neiswanger. Isobench: Benchmarking multimodal foundation models on isomorphic representations. *arXiv preprint arXiv:2404.01266*, 2024.
- [18] Peng Gao, Jiaming Han, Renrui Zhang, Ziyi Lin, Shijie Geng, Aojun Zhou, Wei Zhang, Pan Lu, Conghui He, Xiangyu Yue, et al. Llama-adapter v2: Parameter-efficient visual instruction model. *arXiv preprint arXiv:2304.15010*, 2023.
- [19] Jiuxiang Gu, Chenyang Li, Yingyu Liang, Zhenmei Shi, Zhao Song, and Tianyi Zhou. Fourier circuits in neural networks: Unlocking the potential of large language models in mathematical reasoning and modular arithmetic. *arXiv preprint arXiv:2402.09469*, 2024.
- [20] Kaiming He, Xinlei Chen, Saining Xie, Yanghao Li, Piotr Dollár, and Ross Girshick. Masked autoencoders are scalable vision learners. In *Proceedings of the IEEE/CVF conference on computer vision and pattern recognition*, pages 16000–16009, 2022.
- [21] Muyang He, Yexin Liu, Boya Wu, Jianhao Yuan, Yueze Wang, Tiejun Huang, and Bo Zhao. Efficient multimodal learning from data-centric perspective. *arXiv preprint arXiv:2402.11530*, 2024.
- [22] Wenyi Hong, Weihang Wang, Qingsong Lv, Jiazheng Xu, Wenmeng Yu, Junhui Ji, Yan Wang, Zihan Wang, Yuxuan Zhang, Juanzi Li, Bin Xu, Yuxiao Dong, Ming Ding, and Jie Tang. Cogagent: A visual language model for gui agents. In *Proceedings of the IEEE conference on computer vision and pattern recognition*, 2024.
- [23] Xinyi Hou, Yanjie Zhao, Yue Liu, Zhou Yang, Kailong Wang, Li Li, Xiapu Luo, David Lo, John Grundy, and Haoyu Wang. Large language models for software engineering: A systematic literature review, 2024.
- [24] Michael Igonovitch Ivanitskiy, Rusheb Shah, Alex F. Spies, Tilman Räuher, Dan Valentine, Can Rager, Lucia Quirke, Chris Mathwin, Guillaume Corlouer, Cecilia Diniz Behn, and Samy Wu Fung. A configurable library for generating and manipulating maze datasets, 2023.
- [25] Albert Q Jiang, Alexandre Sablayrolles, Arthur Mensch, Chris Bamford, Devendra Singh Chaplot, Diego de las Casas, Florian Bressand, Gianna Lengyel, Guillaume Lample, Lucile Saulnier, et al. Mistral 7b. *arXiv preprint arXiv:2310.06825*, 2023.
- [26] Justin Johnson, Bharath Hariharan, Laurens Van Der Maaten, Li Fei-Fei, C Lawrence Zitnick, and Ross Girshick. Clevr: A diagnostic dataset for compositional language and elementary visual reasoning. In *Proceedings of the IEEE conference on computer vision and pattern recognition*, pages 2901–2910, 2017.
- [27] Enkelejda Kasneci, Kathrin Seßler, Stefan Küchemann, Maria Bannert, Daryna Dementieva, Frank Fischer, Urs Gasser, Georg Groh, Stephan Günemann, Eyke Hüllermeier, et al. Chatgpt for good? on opportunities and challenges of large language models for education. *Learning and individual differences*, 103:102274, 2023.
- [28] Mehran Kazemi, Hamidreza Alvani, Ankit Anand, Jialin Wu, Xi Chen, and Radu Soricut. Geomverse: A systematic evaluation of large models for geometric reasoning. *arXiv preprint arXiv:2312.12241*, 2023.
- [29] Junnan Li, Dongxu Li, Silvio Savarese, and Steven Hoi. Blip-2: Bootstrapping language-image pre-training with frozen image encoders and large language models. In *International conference on machine learning*, pages 19730–19742. PMLR, 2023.
- [30] Junnan Li, Dongxu Li, Caiming Xiong, and Steven Hoi. Blip: Bootstrapping language-image pre-training for unified vision-language understanding and generation. In *International conference on machine learning*, pages 12888–12900. PMLR, 2022.

- [31] Yinheng Li, Shaofei Wang, Han Ding, and Hang Chen. Large language models in finance: A survey. In *Proceedings of the Fourth ACM International Conference on AI in Finance*, pages 374–382, 2023.
- [32] Yuanzhi Li, Sébastien Bubeck, Ronen Eldan, Allie Del Giorno, Suriya Gunasekar, and Yin Tat Lee. Textbooks are all you need ii: phi-1.5 technical report. *arXiv preprint arXiv:2309.05463*, 2023.
- [33] Weixin Liang, Zachary Izzo, Yaohui Zhang, Haley Lepp, Hancheng Cao, Xuandong Zhao, Lingjiao Chen, Haotian Ye, Sheng Liu, Zhi Huang, et al. Monitoring ai-modified content at scale: A case study on the impact of chatgpt on ai conference peer reviews. *arXiv preprint arXiv:2403.07183*, 2024.
- [34] Haotian Liu, Chunyuan Li, Yuheng Li, and Yong Jae Lee. Improved baselines with visual instruction tuning. *arXiv preprint arXiv:2310.03744*, 2023.
- [35] Haotian Liu, Chunyuan Li, Yuheng Li, Bo Li, Yuanhan Zhang, Sheng Shen, and Yong Jae Lee. Llava-next: Improved reasoning, ocr, and world knowledge, January 2024.
- [36] Haotian Liu, Chunyuan Li, Qingyang Wu, and Yong Jae Lee. Visual instruction tuning. *Advances in neural information processing systems*, 36, 2024.
- [37] Xiao Liu, Zirui Wu, Xueqing Wu, Pan Lu, Kai-Wei Chang, and Yansong Feng. Are llms capable of data-based statistical and causal reasoning? benchmarking advanced quantitative reasoning with data. *arXiv preprint arXiv:2402.17644*, 2024.
- [38] Yuan Liu, Haodong Duan, Yuanhan Zhang, Bo Li, Songyang Zhang, Wangbo Zhao, Yike Yuan, Jiaqi Wang, Conghui He, Ziwei Liu, et al. Mmbench: Is your multi-modal model an all-around player? *arXiv preprint arXiv:2307.06281*, 2023.
- [39] Ze Liu, Han Hu, Yutong Lin, Zhuliang Yao, Zhenda Xie, Yixuan Wei, Jia Ning, Yue Cao, Zheng Zhang, Li Dong, et al. Swin transformer v2: Scaling up capacity and resolution. In *Proceedings of the IEEE/CVF conference on computer vision and pattern recognition*, pages 12009–12019, 2022.
- [40] Ze Liu, Yutong Lin, Yue Cao, Han Hu, Yixuan Wei, Zheng Zhang, Stephen Lin, and Baining Guo. Swin transformer: Hierarchical vision transformer using shifted windows. In *Proceedings of the IEEE/CVF international conference on computer vision*, pages 10012–10022, 2021.
- [41] Pan Lu, Hritik Bansal, Tony Xia, Jiacheng Liu, Chunyuan Li, Hannaneh Hajishirzi, Hao Cheng, Kai-Wei Chang, Michel Galley, and Jianfeng Gao. Mathvista: Evaluating mathematical reasoning of foundation models in visual contexts. *arXiv preprint arXiv:2310.02255*, 2023.
- [42] Brandon McKinzie, Zhe Gan, Jean-Philippe Fauconnier, Sam Dodge, Bowen Zhang, Philipp Dufter, Dhruvi Shah, Xianzhi Du, Futang Peng, Floris Weers, et al. Mm1: Methods, analysis & insights from multimodal llm pre-training. *arXiv preprint arXiv:2403.09611*, 2024.
- [43] Sewon Min, Xinxu Lyu, Ari Holtzman, Mikel Artetxe, Mike Lewis, Hannaneh Hajishirzi, and Luke Zettlemoyer. Rethinking the role of demonstrations: What makes in-context learning work? *arXiv preprint arXiv:2202.12837*, 2022.
- [44] Roshanak Mirzaee, Hossein Rajaby Faghihi, Qiang Ning, and Parisa Kordjmeshidi. Spartqa: A textual question answering benchmark for spatial reasoning. *arXiv preprint arXiv:2104.05832*, 2021.
- [45] Catherine Olsson, Nelson Elhage, Neel Nanda, Nicholas Joseph, Nova DasSarma, Tom Henighan, Ben Mann, Amanda Askell, Yuntao Bai, Anna Chen, et al. In-context learning and induction heads. *arXiv preprint arXiv:2209.11895*, 2022.
- [46] Roma Patel and Ellie Pavlick. Mapping language models to grounded conceptual spaces. In *International conference on learning representations*, 2021.
- [47] William Peebles and Saining Xie. Scalable diffusion models with transformers. In *Proceedings of the IEEE/CVF International Conference on Computer Vision*, pages 4195–4205, 2023.

- [48] Alec Radford, Jong Wook Kim, Chris Hallacy, Aditya Ramesh, Gabriel Goh, Sandhini Agarwal, Girish Sastry, Amanda Askell, Pamela Mishkin, Jack Clark, et al. Learning transferable visual models from natural language supervision. In *International conference on machine learning*, pages 8748–8763. PMLR, 2021.
- [49] Robin Rombach, Andreas Blattmann, Dominik Lorenz, Patrick Esser, and Björn Ommer. High-resolution image synthesis with latent diffusion models. In *Proceedings of the IEEE/CVF conference on computer vision and pattern recognition*, pages 10684–10695, 2022.
- [50] Zhengxiang Shi, Qiang Zhang, and Aldo Lipani. Stepgame: A new benchmark for robust multi-hop spatial reasoning in texts. In *Proceedings of the AAAI conference on artificial intelligence*, pages 11321–11329, 2022.
- [51] Zhenmei Shi, Jiefeng Chen, Kunyang Li, Jayaram Raghuram, Xi Wu, Yingyu Liang, and Somesh Jha. The trade-off between universality and label efficiency of representations from contrastive learning. In *The Eleventh International Conference on Learning Representations*, 2022.
- [52] Zhenmei Shi, Yifei Ming, Ying Fan, Frederic Sala, and Yingyu Liang. Domain generalization via nuclear norm regularization. In *Conference on Parsimony and Learning (Proceedings Track)*, 2023.
- [53] Zhenmei Shi, Junyi Wei, Zhuoyan Xu, and Yingyu Liang. Why larger language models do in-context learning differently? In *R0-FoMo: Robustness of Few-shot and Zero-shot Learning in Large Foundation Models*, 2023.
- [54] Zhongxiang Sun. A short survey of viewing large language models in legal aspect. *arXiv preprint arXiv:2303.09136*, 2023.
- [55] Gemini Team, Rohan Anil, Sebastian Borgeaud, Yonghui Wu, Jean-Baptiste Alayrac, Jiahui Yu, Radu Soricut, Johan Schalkwyk, Andrew M Dai, Anja Hauth, et al. Gemini: a family of highly capable multimodal models. *arXiv preprint arXiv:2312.11805*, 2023.
- [56] Gemma Team, Thomas Mesnard, Cassidy Hardin, Robert Dadashi, Surya Bhupatiraju, Shreya Pathak, Laurent Sifre, Morgane Rivière, Mihir Sanjay Kale, Juliette Love, et al. Gemma: Open models based on gemini research and technology. *arXiv preprint arXiv:2403.08295*, 2024.
- [57] Arun James Thirunavukarasu, Darren Shu Jeng Ting, Kabilan Elangovan, Laura Gutierrez, Ting Fang Tan, and Daniel Shu Wei Ting. Large language models in medicine. *Nature medicine*, 29(8):1930–1940, 2023.
- [58] Hugo Touvron, Thibaut Lavril, Gautier Izacard, Xavier Martinet, Marie-Anne Lachaux, Timothée Lacroix, Baptiste Rozière, Naman Goyal, Eric Hambro, Faisal Azhar, et al. Llama: Open and efficient foundation language models. *arXiv preprint arXiv:2302.13971*, 2023.
- [59] Hugo Touvron, Louis Martin, Kevin Stone, Peter Albert, Amjad Almahairi, Yasmine Babaei, Nikolay Bashlykov, Soumya Batra, Prajjwal Bhargava, Shruti Bhosale, et al. Llama 2: Open foundation and fine-tuned chat models. *arXiv preprint arXiv:2307.09288*, 2023.
- [60] Hugo Touvron, Louis Martin, Kevin Stone, Peter Albert, Amjad Almahairi, Yasmine Babaei, Nikolay Bashlykov, Soumya Batra, Prajjwal Bhargava, Shruti Bhosale, et al. Llama 2: Open foundation and fine-tuned chat models. *arXiv preprint arXiv:2307.09288*, 2023.
- [61] Ashish Vaswani, Noam Shazeer, Niki Parmar, Jakob Uszkoreit, Llion Jones, Aidan N Gomez, Łukasz Kaiser, and Illia Polosukhin. Attention is all you need. *Advances in neural information processing systems*, 30, 2017.
- [62] Weihang Wang, Qingsong Lv, Wenmeng Yu, Wenyi Hong, Ji Qi, Yan Wang, Junhui Ji, Zhuoyi Yang, Lei Zhao, Xixuan Song, Jiazheng Xu, Bin Xu, Juanzi Li, Yuxiao Dong, Ming Ding, and Jie Tang. Cogvlm: Visual expert for pretrained language models, 2023.
- [63] xAI. Grok-1. <https://github.com/xai-org/grok-1>, 2024.

- [64] Zhuoyan Xu, Zhenmei Shi, and Yingyu Liang. Do large language models have compositional ability? an investigation into limitations and scalability. In *ICLR 2024 Workshop on Mathematical and Empirical Understanding of Foundation Models*, 2024.
- [65] Zhuoyan Xu, Zhenmei Shi, Junyi Wei, Fangzhou Mu, Yin Li, and Yingyu Liang. Towards few-shot adaptation of foundation models via multitask finetuning. In *The Twelfth International Conference on Learning Representations*, 2023.
- [66] Yutaro Yamada, Yihan Bao, Andrew Kyle Lampinen, Jungo Kasai, and Ilker Yildirim. Evaluating spatial understanding of large language models. *Transactions on Machine Learning Research*, 2024.
- [67] Qi Zhang, Zhen Lei, Zhaoxiang Zhang, and Stan Z Li. Context-aware attention network for image-text retrieval. In *Proceedings of the IEEE/CVF conference on computer vision and pattern recognition*, pages 3536–3545, 2020.
- [68] Renrui Zhang, Jiaming Han, Aojun Zhou, Xiangfei Hu, Shilin Yan, Pan Lu, Hongsheng Li, Peng Gao, and Yu Qiao. Llama-adapter: Efficient fine-tuning of language models with zero-init attention. *arXiv preprint arXiv:2303.16199*, 2023.
- [69] Renrui Zhang, Dongzhi Jiang, Yichi Zhang, Haokun Lin, Ziyu Guo, Pengshuo Qiu, Aojun Zhou, Pan Lu, Kai-Wei Chang, Peng Gao, et al. Mathverse: Does your multi-modal llm truly see the diagrams in visual math problems? *arXiv preprint arXiv:2403.14624*, 2024.
- [70] Susan Zhang, Stephen Roller, Naman Goyal, Mikel Artetxe, Moya Chen, Shuohui Chen, Christopher Dewan, Mona Diab, Xian Li, Xi Victoria Lin, et al. Opt: Open pre-trained transformer language models. *arXiv preprint arXiv:2205.01068*, 2022.
- [71] Deyao Zhu, Jun Chen, Xiaoqian Shen, Xiang Li, and Mohamed Elhoseiny. Minigpt-4: Enhancing vision-language understanding with advanced large language models. *arXiv preprint arXiv:2304.10592*, 2023.

Appendix

A Limitations and Societal Impact

Limitations. In this work, we introduce three novel benchmarks and conduct a comprehensive evaluation of diverse large language models (LLMs) and vision-language models (VLMs), presenting a controlled and thorough evaluation of spatial reasoning capabilities. While our analysis is detailed and extensive, it remains primarily empirical. We believe that embarking on a formal theoretical study, despite its challenges, would significantly enrich our understanding of pre-trained multimodal language models. Moreover, our focus has been on in-depth analysis rather than on developing new training strategies or adaptation algorithms to enhance spatial reasoning. Recognizing these points, we identify them as valuable directions for future research.

Societal impact. Regarding the positive societal impact, our evaluations and observations could catalyze the development of new algorithms that enhance the spatial reasoning abilities of LLMs and VLMs. Improved understanding of these models has the potential to significantly benefit sectors requiring robust spatial understanding and navigation. This could lead to more reliable and efficient systems that enhance safety and user experience. As for potential negative societal impacts, our work primarily involves empirical evaluations using synthetic datasets designed to probe spatial reasoning. Therefore, we do not anticipate any direct negative societal impacts arising from our current research.

B Experimental Details

B.1 Software and Hardware

Our experiments are conducted on 4 NVIDIA RTX A6000 GPUs (for small-scale models with fewer than 2B parameters) and 4 NVIDIA A100 GPUs (for 7B, 13B, and 34B models). Our implementation is based on Python 3.10 and PyTorch 2.1.2.

B.2 Hyperparameters and Error Bars

The hyperparameters discussed in this paper pertain to the decoding strategies of each model. For deterministic decoding, we adhere to the default settings specified for each model. The models employing deterministic decoding (argmax) include Bunny-Phi-2-SigLIP, CogAgent, CogVLM, InstructBLIP-Vicuna-13B, and InstructBLIP-Vicuna-7B. For non-deterministic decoding, we utilize the default hyperparameters provided by Hugging Face (for instance, Top-P is set at 0.9 and the temperature at 0.2 for LLaVA-1.6). Error bars for the main results (Figure 4) are obtained with three independent runs.

B.3 Model Checkpoints

For most open-source models, we use the checkpoints provided by Hugging Face as shown in Table 1. For Bunny variants (Bunny-Phi-1.5-EVA, Bunny-Phi-1.5-SigLIP and Bunny-Phi-2-EVA), we use merged weights following instructions in <https://github.com/BAAI-DCAI/Bunny/>.

B.4 Detailed Illustration of Datasets

In the main text, we abbreviated the textual descriptions in Figure 1, Figure 2 due to space constraints. In this section, we provide the full descriptions for each task to facilitate a better understanding of spatial reasoning tasks. The complete illustrations are displayed in Figure 13 for Spatial-Map and Figure 14 for Maze-Nav, respectively.

Model Name	Link
LLaMA-2-13B	https://huggingface.co/meta-llama/Llama-2-13b-chat-hf
LLaMA-2-7B	https://huggingface.co/meta-llama/Llama-2-7b-chat-hf
LLaMA-3-8B	https://huggingface.co/meta-llama/Meta-Llama-3-8B-Instruct
Mistral-7B	https://huggingface.co/mistralai/Mistral-7B-Instruct-v0.2
Nous-Hermes-2-Yi-34B	https://huggingface.co/NousResearch/Nous-Hermes-2-Yi-34B
Phi-2	https://huggingface.co/microsoft/phi-2
Vicuna-13B-1.5	https://huggingface.co/lmsys/vicuna-13b-v1.5
Vicuna-7B-1.5	https://huggingface.co/lmsys/vicuna-7b-v1.5
LLaVA-1.6-34B	https://huggingface.co/liuhaotian/llava-v1.6-34b
LLaVA-1.6-Mistral-7B	https://huggingface.co/liuhaotian/llava-v1.6-mistral-7b
LLaVA-1.6-Vicuna-13B	https://huggingface.co/liuhaotian/llava-v1.6-vicuna-13b
LLaVA-1.6-Vicuna-7B	https://huggingface.co/liuhaotian/llava-v1.6-vicuna-7b
Bunny-Phi-2-SigLIP	https://huggingface.co/BAAI/Bunny-v1_0-3B
Qwen-VL	https://huggingface.co/Qwen/Qwen-VL-Chat
CogAgent	https://huggingface.co/THUDM/cogagent-vqa-hf
CogVLM	https://huggingface.co/THUDM/cogv1m-chat-hf
InstructBLIP-Vicuna-13B	https://huggingface.co/Salesforce/instructblip-vicuna-13b
InstructBLIP-Vicuna-7B	https://huggingface.co/Salesforce/instructblip-vicuna-7b

Table 1: Model checkpoints from Hugging Face.



Spatial-Map

TQA
(Text-only)

Consider a map with multiple objects:
Whale's Watches is in the map. Brews Brothers Pub is to the Southeast of Whale's Watches. Himalayan Hot Springs is to the Southeast of Whale's Watches. Himalayan Hot Springs is to the Southeast of Brews Brothers Pub. Dragonfly Drones is to the Southwest of Himalayan Hot Springs. Dragonfly Drones is to the Southeast of Brews Brothers Pub. Unicorn Umbrellas is to the Southwest of Brews Brothers Pub. Unicorn Umbrellas is to the Northwest of Dragonfly Drones. Gale Gifts is to the Northeast of Unicorn Umbrellas. Gale Gifts is to the Southwest of Himalayan Hot Springs.



VQA
(Vision-only)

 The figure represents a map with multiple objects. Each object is associated with a name as shown in the figure.

VTQA
(Vision-text)

 The figure represents a map with multiple objects. Each object is associated with a name as shown in the figure.
The same figure can be described as follows: Whale's Watches is in the map. Brews Brothers Pub is to the Southeast of Whale's Watches. Himalayan Hot Springs is to the Southeast of Whale's Watches. Himalayan Hot Springs is to the Southeast of Brews Brothers Pub. Dragonfly Drones is to the Southwest of Himalayan Hot Springs. Dragonfly Drones is to the Southeast of Brews Brothers Pub. Unicorn Umbrellas is to the Southwest of Brews Brothers Pub. Unicorn Umbrellas is to the Northwest of Dragonfly Drones. Gale Gifts is to the Northeast of Unicorn Umbrellas. Gale Gifts is to the Southwest of Himalayan Hot Springs.

Questions



Q: In which direction is Whale's Watches relative to Dragonfly Drones?
A. Northwest B. Southwest C. Southeast D. Northeast

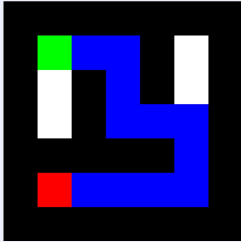
Q: Which object is in the Southwest of Gale Gifts?
A. Dragonfly Drones **B. Unicorn Umbrellas** C. Himalayan Hot Springs D. Brews Brothers Pub

Q: How many objects are in the Southwest of Himalayan Hot Springs?
A. **3** B. 4 C. 1 D. 0

Figure 13: Illustration of the Spatial-Map task with complete textual descriptions in TQA and VTQA.



Maze-Nav



TQA (Text-only)

Here is a Maze represented in ASCII code (LHS), where the symbols have the following meanings:

```
#####
#SXXX#
# #X# #
# #XX# #
#EXXX#
#####
```

- # represents walls that are impassable barriers.
- " " (space) represents the navigable path within the maze, but not necessarily the correct path to the exit.
- S denotes the starting point of the maze.
- E marks the endpoint or the exit of the maze.
- X marks the specific route you should follow to navigate from the starting point 'S' to the endpoint 'E'.
- The objective is to navigate from S to E by following the path marked by X. Movement is allowed in any of the four cardinal directions (up, down, left, right) along the spaces, but to solve the maze, follow the path designated by X.
- A right turn is defined as a change in movement direction that is 90 degrees clockwise relative to the previous direction.
- A left turn is defined as a change in movement direction that is 90 degrees anticlockwise relative to the previous direction.

VQA (Vision-only)

 The figure represents a Maze, where the colored blocks have the following meanings:

- Black blocks represent walls that are impassable barriers.
- White blocks represent navigable paths within the maze, but not necessarily the correct path to the exit.
- Green block denotes the starting point (S) of the maze.
- Red block marks the endpoint or the exit (E) of the maze.
- The objective is to navigate from S to E by following the path marked by Blue. Movement is allowed in any of the four cardinal directions (up, down, left, right) along the White blocks, but to solve the maze, follow the path designated by Blue blocks.
- A right turn is defined as a change in movement direction that is 90 degrees clockwise relative to the previous direction.
- A left turn is defined as a change in movement direction that is 90 degrees anticlockwise relative to the previous direction.

VTQA (Vision-text)

```
#####
#SXXX#
# #X# #
# #XX# #
#EXXX#
#####
```

 The figure represents a Maze, where the colored blocks have the following meanings:

- Black blocks represent walls that are impassable barriers.
- White blocks represent navigable paths within the maze, but not necessarily the correct path to the exit.
- Green block denotes the starting point (S) of the maze.
- Red block marks the endpoint or the exit (E) of the maze.
- The objective is to navigate from S to E by following the path marked by Blue. Movement is allowed in any of the four cardinal directions (up, down, left, right) along the White blocks, but to solve the maze, follow the path designated by Blue blocks.

The same Maze can be represented in ASCII code (LHS), where the symbols have the following meanings:

- # represents walls that are impassable barriers.
- " " (space) represents the navigable path within the maze, but not necessarily the correct path to the exit.
- X marks the specific route you should follow to navigate from the starting point 'S' to the endpoint 'E'.
- S denotes the starting point of the maze.
- E marks the endpoint or the exit of the maze.
- The objective is to navigate from S to E by following the path marked by X. Movement is allowed in any of the four cardinal directions (up, down, left, right) along the spaces, but to solve the maze, follow the path designated by X.

Questions



Q: How many right turns are there in the provided path from S to E?
A. 4 **B. 3** C. 7 D. 2

Q: How many total turns are there in the provided path from S to E?
A. 4 B. 1 C. 9 D. 5

Q: Is the exit directly below the starting point, with no horizontal displacement?
A. Yes B. No

Figure 14: Illustration of the Maze-Nav task with complete textual descriptions in TQA, VQA, and VTQA.

C Further Ablation Studies and Discussions

TQA vs. VTQA: No definitive winner. In Section 4, we demonstrated the advantages of text-only input (TQA) based on LLMs over vision-only input (VQA) based on VLMs. Subsequently, given the same VLM, the comparison between VTQA and VQA in Section 5 reveals that VLMs rely less on visual information when sufficient textual clues are provided. Curious readers seeking a quantitative comparison between TQA and VTQA can refer to the results illustrated in Figure 15. Unlike the other comparisons, no definitive winner emerges between TQA and VTQA across all spatial reasoning tasks, model sizes, and architectures. For instance, the VTQA performance of InstructBLIP-Vicuna-13B surpasses Vicuna-13B in the Maze-Nav task, whereas Vicuna-13B outperforms InstructBLIP-Vicuna-13B in the Spatial-Map task. This indicates that text-only inputs (with language models) still hold an advantage in certain spatial reasoning tasks.

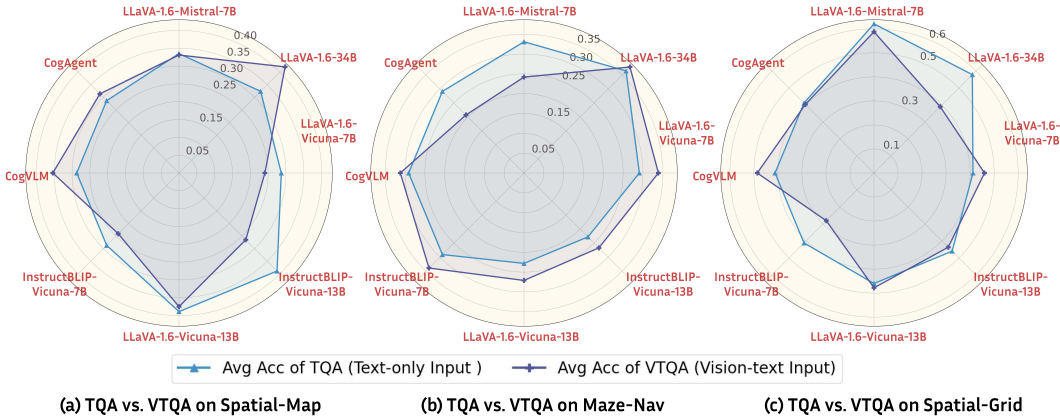


Figure 15: TQA vs. VTQA on spatial reasoning tasks. Each vertex on the spider plot represents the Avg Acc of a (LLM, VLM) pair with the same language model backbone. For LLM, we use the Text-only input (*i.e.*, TQA); for VLM, we use Vision-text input (*i.e.*, VTQA).

D Detailed Experimental Results

In Section 4 and Section 5, to clearly illustrate the impact of modality, we present the results averaged over all questions in Figure 5 for VQA vs. VQA and Figure 10 for VQA vs. VTQA. This section provides a comprehensive breakdown of results for each individual question within the tasks. Detailed comparative results for Spatial-Map, Maze-Nav, and Spatial-Grid are shown in Table 3, Table 4, and Table 5, respectively. We compare language models (LM) and vision-language models (VLM) with the same language model backbone. For the VLM assessments, we consider inputs in both vision-only (VQA) and vision-text (VTQA) formats.

Input Format	Model Name	Spatial-Map Acc	Maze-Nav Acc	Spatial-Grid Acc
Text-only	Claude 3 Opus	0.619	0.277	0.957
	Gemini Pro 1.0	0.453	0.223	0.620
	GPT-4O	0.616	0.353	0.986
	GPT-4V	0.555	0.321	0.923
	GPT-4	0.504	0.353	0.939
Vision-only	Claude 3 Opus	0.348	0.163	0.455
	Gemini Pro 1.0	0.263	0.219	0.512
	GPT-4O	0.617	0.410	0.833
	GPT-4V	0.237	0.263	0.668
Vision-text	Claude 3 Opus	0.606	0.332	0.888
	Gemini Pro 1.0	0.456	0.203	0.687
	GPT-4O	0.643	0.382	0.989
	GPT-4V	0.490	0.333	0.924

Table 2: Detailed results for proprietary models

Input Format	Model Name	Q1 Acc	Q2 Acc	Q3 Acc	Avg Acc
Text-only	Mistral-7B	0.40	0.27	0.34	0.34
	Nous-Hermes-2-Yi-34B	0.45	0.22	0.30	0.32
	Vicuna-7B-1.5	0.39	0.40	0.07	0.29
	Vicuna-13B-1.5	0.44	0.52	0.21	0.39
Vision-only	LLaVA-1.6-Mistral-7B	0.26	0.37	0.13	0.25
	LLaVA-1.6-34B	0.30	0.28	0.30	0.29
	LLaVA-1.6-Vicuna-7B	0.27	0.32	0.26	0.28
	InstructBLIP-Vicuna-13B	0.22	0.21	0.08	0.17
	LLaVA-1.6-Vicuna-13B	0.31	0.32	0.15	0.26
	InstructBLIP-Vicuna-7B	0.25	0.18	0.06	0.16
	CogVLM	0.24	0.39	0.13	0.25
CogAgent	0.29	0.34	0.10	0.25	
Vision-text	LLaVA-1.6-Mistral-7B	0.43	0.42	0.15	0.33
	LLaVA-1.6-34B	0.58	0.47	0.21	0.42
	LLaVA-1.6-Vicuna-7B	0.35	0.25	0.12	0.24
	InstructBLIP-Vicuna-13B	0.39	0.33	0.08	0.27
	LLaVA-1.6-Vicuna-13B	0.49	0.49	0.14	0.38
	InstructBLIP-Vicuna-7B	0.35	0.25	0.12	0.24
	CogVLM	0.40	0.52	0.14	0.35
CogAgent	0.37	0.45	0.12	0.31	

Table 3: Detailed results for the Spatial-Map task. We compare language models (LM) and vision-language models (VLM) with the same language model backbone. For VLMs, we consider both vision-only and vision-text input format. The averaged results are summarized in Figure 5 and Figure 10.

Input Format	Model Name	Q1 Acc	Q2 Acc	Q3 Acc	Avg Acc
Text-only	Mistral-7B	0.43	0.23	0.33	0.33
	Nous-Hermes-2-Yi-34B	0.25	0.18	0.67	0.36
	Vicuna-7B-1.5	0.11	0.13	0.63	0.29
	Vicuna-13B-1.5	0.20	0.15	0.33	0.23
Vision-only	LLaVA-1.6-Mistral-7B	0.25	0.10	0.34	0.23
	LLaVA-1.6-34B	0.27	0.23	0.67	0.39
	LLaVA-1.6-Vicuna-7B	0.17	0.22	0.65	0.35
	InstructBLIP-Vicuna-13B	0.15	0.09	0.67	0.31
	LLaVA-1.6-Vicuna-13B	0.33	0.20	0.33	0.29
	InstructBLIP-Vicuna-7B	0.21	0.28	0.33	0.27
	CogVLM	0.13	0.16	0.66	0.32
CogAgent	0.16	0.22	0.33	0.24	
Vision-text	LLaVA-1.6-Mistral-7B	0.27	0.10	0.36	0.24
	LLaVA-1.6-34B	0.28	0.18	0.68	0.38
	LLaVA-1.6-Vicuna-7B	0.16	0.23	0.63	0.34
	InstructBLIP-Vicuna-13B	0.11	0.11	0.58	0.27
	LLaVA-1.6-Vicuna-13B	0.31	0.18	0.33	0.27
	InstructBLIP-Vicuna-7B	0.16	0.23	0.63	0.34
	CogVLM	0.14	0.20	0.60	0.31
CogAgent	0.14	0.14	0.34	0.21	

Table 4: Detailed results for the Maze-Nav task. We compare language models (LM) and vision-language models (VLM) with the same language model backbone. For VLMs, we consider both vision-only and vision-text input format. The averaged results are summarized in Figure 5 and Figure 10.

Input Format	Model Name	Q1 Acc	Q2 Acc	Q3 Acc	Avg Acc
Text-only	Mistral-7B	0.47	0.73	0.66	0.62
	Nous-Hermes-2-Yi-34B	0.33	0.91	0.50	0.58
	Vicuna-7B-1.5	0.38	0.48	0.38	0.41
	Vicuna-13B-1.5	0.34	0.65	0.39	0.46
Vision-only	LLaVA-1.6-Mistral-7B	0.28	0.69	0.45	0.47
	LLaVA-1.6-34B	0.32	0.29	0.21	0.27
	LLaVA-1.6-Vicuna-7B	0.30	0.38	0.26	0.31
	InstructBLIP-Vicuna-13B	0.24	0.24	0.21	0.23
	LLaVA-1.6-Vicuna-13B	0.30	0.58	0.30	0.40
	InstructBLIP-Vicuna-7B	0.27	0.25	0.24	0.25
	CogVLM	0.25	0.38	0.34	0.32
	CogAgent	0.33	0.33	0.29	0.32
Vision-text	LLaVA-1.6-Mistral-7B	0.32	0.79	0.65	0.59
	LLaVA-1.6-34B	0.44	0.40	0.33	0.39
	LLaVA-1.6-Vicuna-7B	0.36	0.68	0.34	0.46
	InstructBLIP-Vicuna-13B	0.33	0.59	0.39	0.44
	LLaVA-1.6-Vicuna-13B	0.29	0.78	0.36	0.48
	InstructBLIP-Vicuna-7B	0.28	0.29	0.27	0.28
	CogVLM	0.30	0.82	0.35	0.49
	CogAgent	0.33	0.52	0.36	0.40

Table 5: Detailed results for the Spatial-Grid task. We compare language models (LM) and vision-language models (VLM) with the same language model backbone. The averaged results are summarized in Figure 5 and Figure 10.